The International Archives of the Photogrammetry, Remote Sensing and Spatial Information Sciences, Volume XLIX-B3-2026
XXV ISPRS Congress 2026 “From Imagery to Understanding”, Commission III, 4–11 July 2026, Toronto, Canada

A Dual-Task Optimization Approach for Digital Elevation Model Correction with Spaceborne LiDAR Data

Yibo Ling[1], Ting On Chan[1,*], Wing Sum Yan[1]

[1] School of Geography and Planning, Sun Yat-sen University, 510275 Guangzhou, China – (lingyb3, yanws5)@mail2.sysu.edu.cn, chantingon@mail.sysu.edu.cn

Keywords: Spaceborne LiDAR, DEM Correction, Dual-Task Optimization, Deep Learning.

Abstract:

Digital Elevation Models (DEMs) are essential for terrain analysis and environmental applications, yet freely available global DEMs such as the Shuttle Radar Topography Mission (SRTM) DEM often contain noticeable elevation errors. Recent advances in spaceborne LiDAR, particularly Ice, Cloud, and land Elevation Satellite-2 (ICESat-2), provide highly accurate elevation observations for DEM correction. However, most existing studies treat DEM correction as a single regression task and pay limited attention to correction direction, although direction errors may further degrade the corrected DEM. To address this issue, this study proposes a dual-task optimization framework for DEM correction using ICESat-2 data and auxiliary topographic and environmental variables. The network includes a shared feature extraction backbone, a regression branch for estimating correction values, and a classification branch for predicting whether DEM elevation should be increased or decreased. Kent County, New Brunswick, Canada, was selected as the study area, where 35,823 ICESat-2 elevation points were used for model training and validation. Results show that the proposed method outperforms Random Forest, XGBoost, and a conventional deep neural network, achieving a root mean square error (RMSE) of 1.76 m, a mean absolute error (MAE) of 1.37 m, and a direction consistency rate (DCR) of 75.05%. Compared with the original SRTM DEM, the corrected DEM reduces RMSE and MAE by approximately 27.6% and 25.9%, respectively, and improves DCR by 1.66% over the conventional deep neural network (DNN). These results demonstrate that incorporating correction direction into the learning process can effectively improve DEM correction accuracy and directional reliability.

1. Introduction

Digital Elevation Models (DEMs) are fundamental geospatial datasets for a wide range of applications, including hydrological modelling, geomorphological analysis and hazard monitoring (Ling et al., 2024; Wang et al., 2024; Kumar et al., 2023; Pawluszek and Borkowski, 2017). As core representations of terrain morphology, DEMs strongly influence the reliability of topographic analysis and the accuracy of downstream geoscientific inference. Although airborne or unmanned aerial vehicle (UAV)-based Light Detection and Ranging (LiDAR) systems can provide highly accurate elevation data, their deployment over large areas is still expensive, time-consuming, and operationally demanding (Salach et al., 2018). Consequently, freely available global DEM (GDEM) products, such as the Shuttle Radar Topography Mission (SRTM; Farr et al., 2007) DEM, remain widely used because of their extensive spatial coverage and practical accessibility. However, these DEMs often contain non-negligible elevation errors, especially in mountainous and densely vegetated regions, where radar- or image-based elevation retrieval is more vulnerable to terrain occlusion, canopy effects, shadowing, and geometric distortion (Park et al., 2015; Su et al., 2015; Su and Guo, 2014). These limitations can significantly reduce the reliability of terrain characterization in complex environments, making DEM accuracy improvement an important and ongoing research issue.

Recent progress in spaceborne laser altimetry has provided new opportunities for DEM correction. In particular, Ice, Cloud, and land Elevation Satellite-2 (ICESat-2; Abdalati et al., 2010) offers near-global coverage and high vertical accuracy, making it a valuable source of elevation control information. Unlike conventional gridded DEM products, however, ICESat-2 observations are distributed as sparse footprints along orbital tracks rather than as spatially continuous surfaces. This sampling pattern limits their direct use for wall-to-wall DEM generation, but it also creates favourable conditions for data-driven correction strategies (Tian and Shan, 2024). Accordingly, many recent studies have framed DEM correction as a supervised learning problem in which elevation differences between ICESat-2 observations and existing DEMs are treated as target variables, while terrain attributes, land-cover indicators, vegetation information, and environmental variables are used as predictors. Machine learning and deep learning methods have shown strong potential for capturing nonlinear relationships between these variables and spatially distributed DEM errors. For instance, Zhang et al. (2026) used ICESat-2, GEDI, and multisource remote sensing data to correct FABDEM errors in forested regions, while Li et al. (2024) produced a globally corrected DEM product by combining ICESat-2 with land-cover and vegetation information in a random forest framework. At the deep learning level, Chen et al. (2026) developed a CNN–Transformer hybrid model for ICESat-2-based GDEM correction, and Li et al. (2024) proposed a LightGBM-based hybrid framework for forested areas to better disentangle terrain and vegetation effects.

Nevertheless, most existing methods formulate DEM correction primarily as a regression problem and focus on estimating elevation error values. This formulation assumes that the model can adequately learn both the magnitude and direction of correction within a single regression framework. In practice, however, especially in mountainous and heterogeneous terrain, correction direction is a critical aspect of DEM refinement. If the predicted correction direction is incorrect, the adjusted DEM may deviate further from the reference elevation rather than move closer to it. Despite its practical importance, directional information has received limited explicit attention in current DEM.

To address this limitation, this study proposes a dual-task neural network for SRTM DEM correction using ICESat-2

https://doi.org/10.5194/isprs-archives-XLIX-B3-2026-177-2026

observations and auxiliary topographic and environmental variables. The framework consists of a shared feature-learning backbone followed by two task-specific tasks: a classification task that predicts whether DEM elevation should be increased or decreased, and a regression task that estimates the correction value. The auxiliary direction prediction task is introduced to improve the model’s sensitivity to correction direction, thereby assisting the main regression task in producing more reliable DEM correction estimates. In addition, a hybrid loss function is designed to optimize the main regression task while introducing directional classification as an auxiliary supervision signal during training. By incorporating correction direction into the learning process, the proposed framework is expected to enhance the stability and reliability of DEM error estimation in complex mountainous areas, thereby providing a more effective strategy for refining global DEM products.

2. Study area and data

Kent County, located in New Brunswick, Canada, was selected as the study area (Figure 1). The region covers approximately 4,550 km^2 and has an elevation range of -20 to 107 m. Within this area, 35,823 ICESat-2 elevation points were available, providing a sufficiently dense set of reference observations for DEM error modelling and validation. The region is characterized by low-relief terrain interspersed with wetlands, forested areas, and cultivated land, where subtle elevation variations are crucial for accurate terrain representation. Under such conditions, errors in the SRTM DEM may introduce local distortions in surface morphology and increase the difficulty of determining the appropriate correction direction, particularly in flat or gently undulating areas. The diverse land-cover and terrain characteristics of the region therefore provide a suitable test bed for evaluating the robustness and generalization capacity of the proposed direction-constrained DEM correction framework.

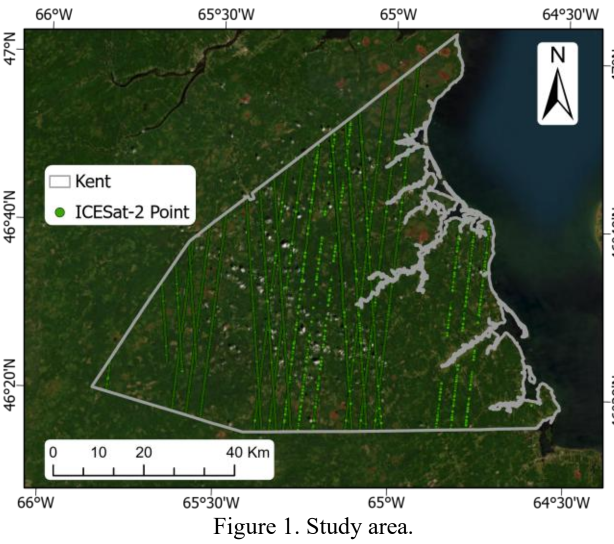

Figure 1. Study area.

In addition, this study will incorporate topographic factors derived from the original DEM, including slope, aspect, curvature, profile curvature, and planar curvature, together with environmental factors such as normalized difference vegetation index (NDVI), fractional vegetation cover (FVC), and landcover, as preliminary candidate variables for screening. Airborne LiDAR point cloud data obtained from the GeoNB Spatial Data Infrastructure platform will be used as the reference elevation dataset for evaluation.

3. Method

The proposed method aims to correct SRTM DEM elevation errors by integrating ICESat-2 altimetry observations with topographic and environmental predictors through a dual-task neural network. The core idea is to formulate DEM correction as a primary regression task supported by an auxiliary correction direction prediction task. Instead of relying solely on direct regression of elevation differences, the proposed framework introduces an auxiliary direction prediction task to provide additional supervision during training. The main regression task remains responsible for estimating the DEM correction value, while the auxiliary branch helps the model better capture directional characteristics of elevation errors.

The overall workflow consists of four stages. First, the SRTM DEM, ICESat-2 elevation measurements, and auxiliary terrain-related variables are unified under a common coordinate system and spatial resolution. Candidate influencing factors are initially selected, and key variables are subsequently identified through Spearman correlation analysis (Spearman, 1987) for model input. Second, the elevation difference between ICESat-2 observations and the SRTM DEM is calculated as the target correction value. Third, a shared deep neural network is used to learn common feature representations from the selected input variables, after which two task-specific branches are employed to predict the correction direction and correction value, respectively. Finally, the predicted correction value is applied to the original SRTM DEM to generate the corrected elevation surface.

This design explicitly incorporates directional constraints into the DEM correction process, thereby reducing the risk of sign-inconsistent predictions that may otherwise degrade DEM accuracy.

3.1 Spearman correlation analysis

To quantify the associations between candidate topographic and environmental variables and SRTM DEM errors, and to identify features with meaningful explanatory potential, a Spearman rank correlation analysis was performed prior to model construction. After pre-processing, the raster values of all candidate predictors were extracted at the ICESat-2 sampling locations and paired with the corresponding elevation differences between ICESat-2 observations and the SRTM DEM. These paired samples were then ranked feature by feature, and the Spearman correlation coefficient is defined as (Al-Hameed and Khawla, 2022):

$$\rho = 1 - \frac{6\sum d_i^2}{n(n^2-1)} \tag{1}$$

where d_i represents the difference between the ranks of the i-th sample for the two variables being compared, and n denotes the total number of samples. As a nonparametric measure of association, Spearman correlation is suitable for characterizing monotonic relationships between variables without imposing strict assumptions of linearity or normality, which makes it particularly appropriate for heterogeneous terrain and environmental data.

3.2 Sample construction and target definition

To build the training samples, ICESat-2 elevation observations are used as high-accuracy elevation control points. For each

https://doi.org/10.5194/isprs-archives-XLIX-B3-2026-177-2026 |

valid ICESat-2 footprint, the corresponding SRTM DEM elevation and auxiliary predictor variables are extracted. The correction target is defined as the elevation difference between the reference elevation and the original DEM:

$$\Delta h_i = h_i^{\text{ref}} - h_i^{\text{SRTM}}, \tag{2}$$

where h_i^{ref} denotes the reference elevation derived from ICESat-2 at sample i, and h_i^{SRTM} denotes the corresponding SRTM elevation. A positive Δh_i indicates that the SRTM DEM underestimates the terrain elevation and should be increased, whereas a negative Δh_i indicates that the SRTM DEM overestimates the terrain elevation and should be decreased. Based on this definition, the DEM correction problem is decomposed into two learning targets: direction label and correction value. The correction direction is formulated as a binary classification task:

$$y_i^c = \begin{cases} 1, & \Delta h_i > 0, \\ 0, & \Delta h_i \le 0, \end{cases} \tag{3}$$

where y_i^c represents the directional label of sample i. The numerical elevation difference Δh_i is used as the regression target for magnitude estimation. Through this formulation, the model learns not only the continuous variation of DEM error but also the categorical decision of whether the terrain elevation should be corrected upward or downward.

3.3 Dual-Task Framework

To jointly model correction direction and value, a dual-Task neural network is proposed. The network consists of a shared feature extraction backbone and two task-specific output branches (Figure 2).

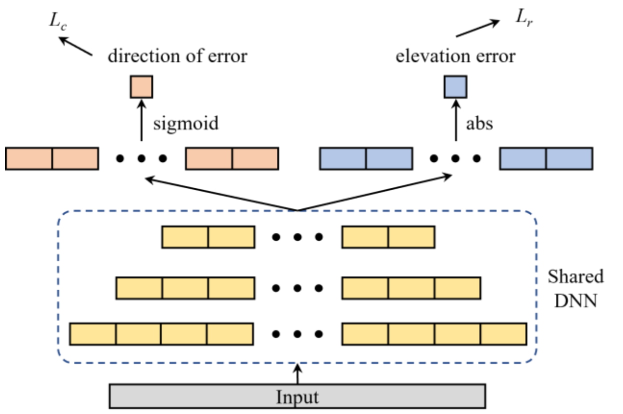

Figure 2. The structure of dual-task neural network.

Given an input feature vector x_i for sample i, the shared backbone first maps the raw predictors into a latent feature space:

$$\mathbf{z}_i = f_\theta(\mathbf{x}_i), \tag{4}$$

where $f_\theta(\cdot)$ denotes the shared deep neural network parameterized by θ, and $\mathbf{z}_i$ is the learned high-level representation. The shared backbone is designed to capture the common relationships between terrain/environmental attributes and DEM error characteristics.

In this study, the backbone is implemented as a multilayer fully connected neural network. Such a structure is suitable for tabular geospatial predictors and enables nonlinear feature interaction learning without requiring manually specified rules. The first branch is responsible for predicting the correction direction. It takes the shared feature representation $\mathbf{z}_i$ as input and outputs the probability that the correction should be positive:

$$p_i = g_\phi(\mathbf{z}_i), \tag{5}$$

where $g_\phi(\cdot)$ denotes the classification branch parameterized by ϕ, and $p_i \in [0,1]$ represents the probability of a positive correction. A larger p_i indicates a higher likelihood that the SRTM DEM should be increased at that location. The predicted direction can be written as:

$$\hat{y}_i^c = \begin{cases} 1, & p_i > 0.5, \\ 0, & p_i \le 0.5. \end{cases} \tag{6}$$

The second branch estimates the correction value required for DEM adjustment $\mathbf{z}_i$ and produces a continuous output:

$$v_i = r_\psi(\mathbf{z}_i), \tag{7}$$

where $r_\psi(\cdot)$ denotes the regression branch parameterized by ψ, and v_i is the predicted correction value. This branch aims to learn the DEM elevation error from the input predictors in a continuous manner. Accordingly, the corrected DEM elevation is computed as:

$$\hat{h}_i^{\text{corr}} = h_i^{\text{SRTM}} + \Delta\hat{h}_i. \tag{8}$$

This formulation ensures that the final correction is not determined solely by the regression branch, but is explicitly constrained by the predicted direction. As a result, the model is better able to reduce sign-inconsistent corrections that may otherwise degrade DEM accuracy.

3.4 Dual-task loss function

Since the proposed framework simultaneously performs classification and regression, a joint optimization strategy is adopted. The total loss is defined as a weighted combination of classification loss and regression loss:

$$L = \lambda_c L_c + \lambda_r L_r, \tag{9}$$

where L_c and L_r denote the classification and regression losses, respectively, and λ_c and λ_r are their corresponding weights. To improve the prediction of correction direction, the direction branch is trained using a weighted loss function, in which different weights are assigned to positive and negative correction samples to alleviate the effect of class imbalance. The loss is defined as:

$$L_c = -\frac{1}{N}\sum_{i=1}^{N} \alpha_i \log(p_{t,i}), \tag{10}$$

https://doi.org/10.5194/isprs-archives-XLIX-B3-2026-177-2026 | © Author(s) 2026. CC BY 4.0 License.

where N is the number of samples, $p_{t,i}$ is the predicted probability corresponding to the true class of sample i, α_i is the class weight. By assigning different weights to positive and negative correction samples, the weighted classification loss alleviates the effect of class imbalance and improves the robustness of correction direction prediction. For the regression branch, the loss is defined as the mean squared error between the predicted correction value and the reference correction value:

$$L_r = \frac{1}{N}\sum_{i=1}^{N}\left(\Delta\hat{h}_i - \Delta h_i\right)^2. \tag{11}$$

This term encourages the predicted correction to approximate the true elevation difference numerically.

4. Experiments

To verify the effectiveness of the proposed framework, a series of comparative experiments were conducted using several representative baseline models, including Random Forest (RF), Extreme Gradient Boosting (XGBoost), and a conventional deep neural network (DNN). To ensure a fair comparison, all baseline models were optimized through hyperparameter tuning, and their best parameter settings were used in the final experiments. Model performance was evaluated using root mean square error (RMSE), mean absolute error (MAE), and direction consistency rate (DCR), thereby assessing both the numerical accuracy of the predicted correction values and the directional reliability of the predicted corrections. Specifically, RMSE and MAE measure the discrepancy between the predicted and reference correction values, where RMSE places greater emphasis on large errors and MAE reflects the average absolute deviation in a more intuitive manner. DCR is used to evaluate whether the predicted correction direction agrees with the reference direction, and a higher DCR indicates better directional consistency and a lower risk of sign-inconsistent DEM corrections. The metrics are defined as follows:

$$RMSE = \sqrt{\frac{1}{N}\sum_{i=1}^{N}(h_i - \hat{h}_i)^2}\ , \tag{12}$$

$$MAE = \frac{1}{N}\sum_{i=1}^{N}\left|h_i - \hat{h}_i\right|, \tag{13}$$

$$DCR = \frac{1}{N}\sum\nolimits_{i=1}^{N} I\left(\hat{d}_i \cdot d_i = 1\right),\ \hat{d}_i, d_i \in \{1,-1\}, \tag{14}$$

where $\hat{h}_i$ and h_i denote the predicted and reference correction values for the i-th sample, respectively; N is the total number of samples; and $I(\cdot)$ is an indicator function that equals 1 when the predicted and reference correction directions are consistent, and 0 otherwise.

5. Results

5.1 Spearman correlation analysis

Figure 3 shows the Spearman correlation matrices of terrain and environmental variables. In each matrix, the lower triangular part presents the pairwise correlation coefficients, whereas the upper triangular part gives the corresponding significance levels (p-values). The results indicate that most feature pairs are statistically significant at the 95% confidence level (p<0.05), suggesting that the selected variables are meaningfully associated with each other and with DEM error to varying degrees.

A closer examination of the correlation patterns reveals several noteworthy relationships. Among the topographic variables, slope and relief amplitude exhibit highly consistent correlations with elevation bias, with similar coefficient signs and comparable magnitudes, implying that they capture partially overlapping information related to terrain undulation. Likewise, among the vegetation-related factors, FVC and NDVI show similar correlation structures and nearly consistent trends with other variables, indicating substantial redundancy in their representation of vegetation conditions.

To avoid interference from redundant information during model construction and to ensure the representativeness and independence of the input features, slope and FVC were ultimately selected as the core influencing factors based on the above correlation analysis. This selection was motivated not only by their significant associations revealed in the correlation analysis, but also by extensive evidence from previous studies (Li et al., 2024a; Magruder et al., 2021), which has confirmed their effectiveness in supporting subsequent analysis and DEM error modelling.

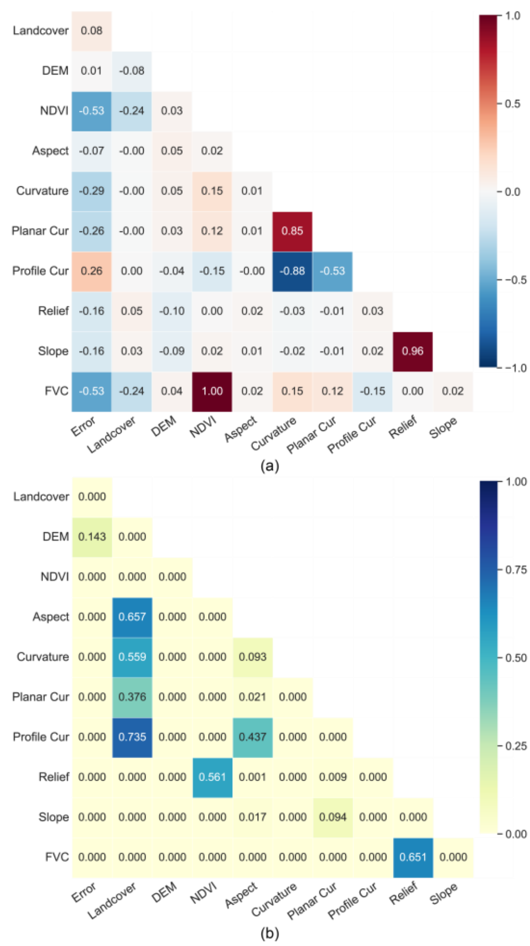

Figure 3. Result of the Spearman correlation analysis. (a) Correlation matrix. (b) P-value matrix.

https://doi.org/10.5194/isprs-archives-XLIX-B3-2026-177-2026

5.2 Accuracy Assessment of the Corrected DEM

The comparison of DEM correction performance is presented in Table X. Relative to the uncorrected DEM, all four data-driven methods reduced prediction errors to varying degrees, demonstrating the feasibility of learning DEM correction patterns from ICESat-2 observations and auxiliary predictors. The proposed method achieved the best performance among all competing approaches, with an RMSE of 1.76 m, an MAE of 1.37 m, and a DCR of 75.05%. Compared with the original SRTM DEM, this corresponds to reductions of approximately 27.6% in RMSE and 25.9% in MAE, highlighting the effectiveness of the correction framework.

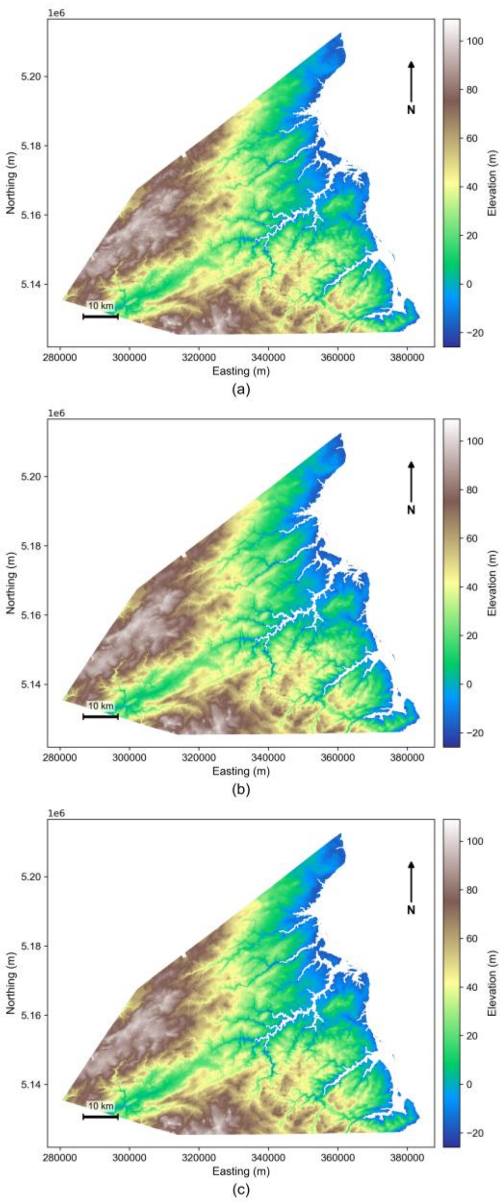

Figure 4. Visual comparison of DEM. (a) Origin DEM. (b) Reference DEM. (c) Corrected DEM by our method.

Notably, the proposed dual-task neural network also outperformed the conventional single-task DNN, indicating that the performance gain did not arise solely from model depth, but from the introduction of the auxiliary correction direction task. Specifically, compared with the DNN, the proposed method reduced RMSE from 1.81 m to 1.76 m and MAE from 1.42 m to 1.37 m, while increasing DCR from 73.39% to 75.05%, i.e., by approximately 1.66 percentage points. By jointly learning correction magnitude and correction direction, the network was encouraged to extract more discriminative representations of DEM error patterns. The direction prediction branch provided additional supervisory information that helped the shared feature extractor better characterize whether the observed bias was positive or negative, which in turn improved the accuracy of the final regression output. The superior DCR further confirms that the auxiliary task enhanced the model’s ability to generate directionally consistent corrections. Overall, these results verify the effectiveness of the proposed dual-task design for DEM error correction.

Table 1. Evaluation results of DEM correction using different methods.

	RMSE	MAE	DCR
RF	1.92	1.49	72.61%
XGBoost	1.92	1.48	72.78%
DNN	1.81	1.42	73.39%
Our method	**1.76**	**1.37**	**75.05%**
No correction	2.43	1.85	--

From a visual perspective (Figure 4), the differences between the original DEM and the corrected DEM are not readily distinguishable. This is likely because the study area is characterized by relatively low-relief terrain, where elevation variations are generally subtle and the magnitude of DEM correction is limited.

6. Conclusion

This study proposed a dual-task optimization framework for SRTM DEM correction using ICESat-2 elevation observations and auxiliary terrain-related variables. Unlike conventional DEM correction methods that rely solely on regression, the proposed approach explicitly incorporates correction direction as an auxiliary classification task, allowing the model to jointly learn both the magnitude and sign of elevation correction. This design improves the model’s sensitivity to directionally consistent DEM adjustments and reduces the risk of sign-inconsistent predictions.

Using Kent County in New Brunswick, Canada, as the study area, the proposed framework demonstrated clear advantages over several representative baseline methods, including Random Forest, XGBoost, and a conventional DNN. The corrected DEM produced by the proposed method achieved the best overall performance, with an RMSE of 1.76 m, an MAE of 1.37 m, and a DCR of 75.05%. Compared with the original SRTM DEM, the method reduced RMSE by approximately 27.6% and MAE by 25.9%. In addition, compared with the single-task DNN, the dual-task design further improved both numerical accuracy and directional consistency, confirming that the auxiliary direction prediction task contributed meaningful supervisory information to DEM error modelling.

The results indicate that introducing directional constraints into the DEM correction process is an effective way to enhance the reliability of correction estimates derived from sparse space-borne LiDAR observations. The proposed framework is particularly suitable for DEM refinement tasks in areas where accurate determination of correction direction is important for preserving terrain realism. Future work will further examine the transferability of the method across different geomorphological regions and DEM products, and explore the integration of additional multisource predictors and spatial context information to further improve large-scale DEM correction performance.

Acknowledgements

This research was funded by the Science and Technology Program of Guangzhou, China (202201011686)

References

Abdalati, W., Zwally, H.J., Bindschadler, R., Csatho, B., Farrell, S.L., Fricker, H.A., Harding, D., Kwok, R., Lefsky, M. and Markus, T., 2010. The ICESat-2 laser altimetry mission. *Proceedings of the IEEE*, 98(5), 735–751.

Al-Hameed, A.A. and Khawla, 2022. Spearman's correlation coefficient in statistical analysis. *International Journal of Nonlinear Analysis and Applications*, 13(1), 3249–3255.

Chen, J., Xiong, L., Li, S., Tang, G. and Strobl, J., 2026. Integrating Neighboring Structure Knowledge Into a CNN-Transformer Hybrid Model for Global Open-Access DEM Correction Using ICESat-2 Altimetry. *IEEE Transactions on Geoscience and Remote Sensing*, 64, 1–20.

Farr, T.G., Rosen, P.A., Caro, E., Crippen, R., Duren, R., Hensley, S., Kobrick, M., Paller, M., Rodriguez, E. and Roth, L., 2007. The shuttle radar topography mission. *Reviews of geophysics*, 45(2).

Kumar, V., Sharma, K.V., Caloiero, T., Mehta, D.J. and Singh, K., 2023. Comprehensive Overview of Flood Modeling Approaches: A Review of Recent Advances. *Hydrology*, 10(7), 141.

Li, B., Xie, H., Liu, S., Ye, Z., Hong, Z., Weng, Q., Sun, Y., Xu, Q. and Tong, X., 2024a. Global DEM Product Generation by Correcting ASTER GDEM Elevation with ICESat-2 Altimeter Data. *Earth System Science Data Discussions*, 1–24.

Li, Q., Wang, D., Liu, F., Yu, J. and Jia, Z., 2024b. LightGBM hybrid model based DEM correction for forested areas. *PloS One*, 19(10), e0309025.

Ling, Y., Wang, Y., Lin, Y., Chan, T.O. and Awange, J., 2024. Optimized Landslide Segmentation From Satellite Imagery Based on Multiresolution Fusion and Attention Mechanism. *IEEE Geoscience and Remote Sensing Letters*, 21, 1–5.

Magruder, L., Neuenschwander, A. and Klotz, B., 2021. Digital terrain model elevation corrections using space-based imagery and ICESat-2 laser altimetry. *Remote Sensing of Environment*, 264, 112621.

Park, W., Sohn, H.-G. and Heo, J., 2015. Estimation of forest canopy height using orthoimage-refined digital elevation models. *Landscape and Ecological Engineering*, 11(1), 73–86.

Pawluszek, K. and Borkowski, A., 2017. Impact of DEM-derived factors and analytical hierarchy process on landslide susceptibility mapping in the region of Rożnów Lake, Poland. *Natural Hazards*, 86(2), 919–952.

Salach, A., Bakuła, K., Pilarska, M., Ostrowski, W., Górski, K. and Kurczyński, Z., 2018. Accuracy Assessment of Point Clouds from LiDAR and Dense Image Matching Acquired Using the UAV Platform for DTM Creation. *ISPRS International Journal of Geo-Information*, 7(9), 342.

Spearman, C., 1987. The Proof and Measurement of Association between Two Things. *The American Journal of Psychology*, 100(3/4), 441–471.

Su, Y. and Guo, Q., 2014. A practical method for SRTM DEM correction over vegetated mountain areas. *ISPRS Journal of Photogrammetry and Remote Sensing*, 87, 216–228.

Su, Y., Guo, Q., Ma, Q. and Li, W., 2015. SRTM DEM Correction in Vegetated Mountain Areas through the Integration of Spaceborne LiDAR, Airborne LiDAR, and Optical Imagery. *Remote Sensing*, 7(9), 11202–11225.

Tian, X. and Shan, J., 2024. ICESat-2 Controlled Integration of GEDI and SRTM Data for Large-Scale Digital Elevation Model Generation. *IEEE Transactions on Geoscience and Remote Sensing*, 62, 1–14.

Wang, Y., Ling, Y., Chan, T.O. and Awange, J., 2024. High-resolution earthquake-induced landslide hazard assessment in Southwest China through frequency ratio analysis and LightGBM. *International Journal of Applied Earth Observation and Geoinformation*, 131, 103947.

Zhang, Y., Huang, J., Liang, L. and Mo, F., 2026. A Hierarchical Optimization Model Based on Multisource Remote Sensing to Correct FABDEM. *IEEE Journal of Selected Topics in Applied Earth Observations and Remote Sensing*, 19, 5267–5282.